Journal of Zhejiang University SCIENCE B
ISSN 1673-1581 (Print); ISSN 1862-1783 (Online)
www.zju.edu.cn/jzus; www.springerlink.com
E-mail: jzus@zju.edu.cn

Representing the retinal line spread shape with mathematical functions*

Yi-rong YANG[†‡1,2], Justin WANEK[2], Mahnaz SHAHIDI[2]

([1]*Department of Bioengineering, University of Illinois at Chicago, IL 60607, USA*)

([2]*Department of Ophthalmology and Visual Sciences, University of Illinois at Chicago, IL 60607, USA*)

[†]E-mail: yyang19@uic.edu

Received June 5, 2008; revision accepted Aug. 17, 2008; CrossCheck deposited Oct. 29, 2008

Abstract: Objective: To report a mathematical function that characterizes the double-pass line spread function (LSF) of the human eye. Determining analytical functions that represent the double-pass LSF is important because it allows modeling the optical performance of the eye. Methods: Optical section retinal images, generated in normal human eyes using a modified slit-lamp biomicroscope, were analyzed to derive the double-pass LSF by plotting the intensity distribution of laser light reflected/scattered from the vitreoretinal interface. Three mathematical functions (Lorentzian, Gaussian, exponential) were fitted to the double-pass LSF and the root mean square error (RMSE) was calculated to provide a measure of the goodness of fit. Results: The Lorentzian function provided the best representation of the double-pass LSF of normal human eyes. The full width at half maximum (FWHM) of the Lorentzian fitted curve was positively correlated with age, indicating that the double-pass LSF broadens with age. Furthermore, the goodness of fit of the Lorentzian function was significantly better in younger subjects as compared with older subjects, suggesting that the fitted function to the double-pass LSF may vary according to age. Conclusion: The results demonstrate an age-related change in the double-pass LSF width and the goodness of fit of the Lorentzian function.

Key words: Retina, Double-pass line spread function (LSF), Lorentzian, Gaussian, Exponential
doi:10.1631/jzus.B0820184 **Document code:** A **CLC number:** Q81

INTRODUCTION

Imperfections in the optics of the eye effectively cause light to spread across the retina, thus preventing the formation of a perfect point image from a point source. Accordingly, one fundamental measure of the optical quality of the human eye is the distribution of light intensity on the retina from a line or point source. By providing a measure of the spread of light on the retina, the point spread function (PSF) or line spread function (LSF), imparts information about the optical performance of the human eye.

There are two established techniques for determining the PSF and LSF of the human eye. Wavefront measurement techniques utilize instruments, such as a Shack-Hartmann sensor or cross-cylinder aberroscope, to spatially resolve the wavefront aberrations of the eye. The PSF is derived mathematically (not physically measured) from the wavefront aberration function, and therefore accounts for only aberrations and diffraction, and not for scatter (Chen *et al*., 2005; Collins *et al*., 2006). The double-pass technique captures an image of a point or line source projected on the retina and thus produces a PSF or LSF that incorporates the contributions of aberrations, diffraction, and scatter (Westheimer and Liang, 1994; Iglesias *et al*., 1998; Guirao *et al*., 1999; Diaz-Douton *et al*., 2006). The intensity profile is quantified by averaging the radial intensity distribution over all meridians of a two-dimensional PSF (Liang and Westheimer, 1995; Iglesias *et al*., 1998),

‡ Corresponding author

* Project supported by the National Eye Institute, Bethesda, MD (Nos. EY14275 and EY1792), Department of Veteran Affairs, and the Research to Prevent Blindness, UIC Eye Center, New York, NY, USA

whereas the LSF is determined by generating intensity profiles across a line image (Flamant, 1955; Jones, 1958; Westheimer and Campbell, 1962; Westheimer, 1963; Campbell and Gubisch, 1966; Karbassi *et al*., 1993). Several modifications of the double-pass technique have also been developed (Artal *et al*., 1995a; Navarro and Losada, 1995) including our method in which a laser is obliquely projected and the double-pass LSF is derived based on reflection/scattering of laser light from the retinal interfaces (Shahidi *et al*., 2004).

The PSF represents the spread of light in two dimensions, whereas the LSF measures light distribution in only one dimension and thus can be simply represented by a one-dimensional function. Traditionally, the LSF has been fitted with exponential functions (Flamant, 1955; Westheimer and Campbell, 1962); however, to our knowledge a statistical comparison of the double-pass LSF fitted with different mathematical functions has not been undertaken. Characterizing the double-pass LSF using a mathematical function provides an accurate model and description of the optical performance of the eye, and allows an analytical expression to be derived for the modulation transfer function (MTF).

The purpose of the current study was to determine a mathematical function that best-fits the experimentally derived double-pass LSF in normal human eyes. Additionally, the presence of a change in the goodness of fit due to aging was investigated. The double-pass LSF was derived using our previously reported imaging technique (Shahidi and Yang, 2004) and fitted with three mathematical functions (Lorentzian, Gaussian, exponential), commonly used to describe laser profiles (Röhler and Howland, 1979; David, 1996; Yin *et al*., 2003; Peng and Lu, 2005).

METHODS

Imaging

The optical section imaging system has been described previously (Shahidi *et al*., 2004). Briefly, the instrument consisted of a slitlamp biomicroscope that was modified to deliver a 543-nm helium neon laser beam to the eye and a charge-coupled device (CCD) camera that captures images. The laser beam was expanded and then projected through the optics of the slitlamp, a cylindrical lens, and a Volk front lens. The beam was focused by the optics of the eye to a line on the retina, within 500 μm of the fovea. Light reflected and scattered from the anterior and posterior retinal surfaces was imaged by the optics of the slitlamp, and an optical section image was captured by a CCD camera attached to the arm of the slitlamp.

The incident laser beam entered the eye horizontally displaced from the pupil center. The reflected light from the retina was imaged through the opposite side of the pupil, and thus the pupil did not form the aperture stop for imaging. Due to the stereobase angle (~10°) between the incident laser and imaging axis, on the optical section image, retinal structures appeared laterally displaced according to their depth location. The optical section image was primarily composed of two laterally displaced lines, corresponding to the reflection and/or scattering of the laser light from the vitreoretinal and chorioretinal interfaces.

Subjects

Imaging was performed in 1 eye of each of 21 normal healthy subjects, with ages between 23 and 70 years and an average age of (46±16) years (mean±*SD*). Patients with retinitis pigmentosa (RP) had 20/50 or better best-corrected visual acuities in the tested eyes and had minimal or no clinically visible posterior subcapsular cataract (PSC) cataract as evaluated by slitlamp biomicroscopy. The patients with RP in the current study were a subset of those from a previous study in which ocular higher-order aberrations were measured using a different wavefront sensing instrument. The control subjects had best-corrected visual acuities of 20/20 or better in the tested eye, no history of ocular disease, and a normal ophthalmic examination. Subjects with more than minimal nuclear or cortical cataracts, or refractive errors >5 diopters, were not included in the study. Prior to imaging, the study was described to the subjects, and informed consent was obtained according to the tenets of the Declaration of Helsinki. The subject's pupil was dilated with 2.5% (w/v) phenylephrine hydrochloride and 1% (w/v) tropicamide to approximately 6 mm, and his/her head was stabilized with a head and chin rest. Prior to imaging, low order aberrations (defocus) were corrected by moving the front lens, which was mounted on a linear translation stage, while simultaneously viewing

the optical section image on a video monitor. The position of the front lens was fixed when the image appeared best focused. In a previous study, optical section images in 15 out of these 21 subjects were analyzed and the area under the light spread function was reported (Shahidi *et al*., 2004).

Section image processing and analysis

A dedicated software program was developed using Matlab (the MathWorks, Inc., Natick, MA, USA) to process and analyze the optical section images. For each optical section image, a central segment of 120 (vertical)×480 (horizontal) pixels was vertically averaged to generate an intensity profile. The vertical dimension corresponded to a distance of 500 μm on the retina. Fig.1a shows a typical example of an optical section retinal image, cropped to depict the area of interest, obtained in one subject in the study. The intensity profile derived from the image displayed two distinct peaks, corresponding to light reflected/scattered from the vitreoretinal (anterior) and chorioretinal (posterior) interfaces. The intensity profile was differentiated and the location of the peak corresponding to the vitreoretinal interface was identified. The double-pass LSF was derived by mirroring the intensity distribution about the peak and thus creating a symmetric function (Fig.1b). The LSF was normalized by first subtracting the mean background intensity and then being divided by the difference between the maximum intensity and mean background intensity. The tails of the normalized LSF were truncated by determining the location at which the LSF became zero (equal to the background intensity). This location from one side of the peak occurred at a distance of (48±11) arc min (mean±*SD*, *N*=21). Therefore, the central part of the double-pass LSF, which was governed primarily by aberrations and diffraction, was taken into account (Ijspeert *et al*., 1990; Beckman *et al*., 1994; van den Berg, 1995; Westheimer and Liang, 1995).

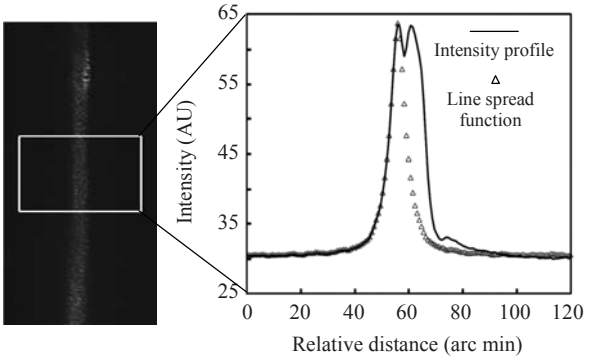

Fig.1 (a) Example of an optical section retinal image obtained in one subject. An intensity profile was derived from the area of interest outlined by the rectangular box; (b) Example of an intensity profile, obtained from the area outlined in (a). The left and right peaks coincide with the vitreoretinal and chorioretinal interfaces, respectively. The line spread function was derived by mirroring the left side of the intensity distribution about its peak

Curve fitting functions

The LSF was fitted with three different mathematical functions: Lorentzian, Gaussian, and exponential. These mathematical functions were selected, since they are frequently used to describe laser profiles and light distribution patterns. The normalized Lorentzian function was defined by Eq.(1), where the parameter Γ specifies the full width at half maximum (FWHM) and x_0 is the horizontal coordinate of the peak:

$$I(x) \sim \frac{(\Gamma/2)^2}{(x-x_0)^2+(\Gamma/2)^2}. \tag{1}$$

The normalized Gaussian function was described by Eq.(2), where the parameter σ is the standard deviation (*SD*):

$$I(x) \sim \exp\left[-\frac{(x-x_0)^2}{2\sigma^2}\right]. \tag{2}$$

The normalized exponential function was defined by Eq.(3), where b is the exponential decay constant:

$$I(x) \sim \exp\left(-\frac{|x-x_0|}{b}\right). \tag{3}$$

A Matlab program was written to fit the LSF with each of the three functions using a linear least square technique. Location of x_0 was fixed to the measured LSF peak location, whereas values of Γ, σ, and b that minimized the square error of the functions were determined. Parameters obtained from three images in each subject were averaged. The central LSF and the peripheral LSF were equally considered for curve

fitting. Thus, the parameters of the best fitting functions can reflect both aberrations and scatter changes. Examples of the same LSF fitted with each of the three mathematical functions are shown in Fig.2. The shapes of the three fitted functions are similar, each having a maximum intensity at x_0. However, differences in their shapes exist. The exponential function has the sharpest peak with non-zero slope as compared with the Lorentzian and Gaussian functions, whereas the Lorentzian function has a more gradual decline at the base as compared with the Gaussian function.

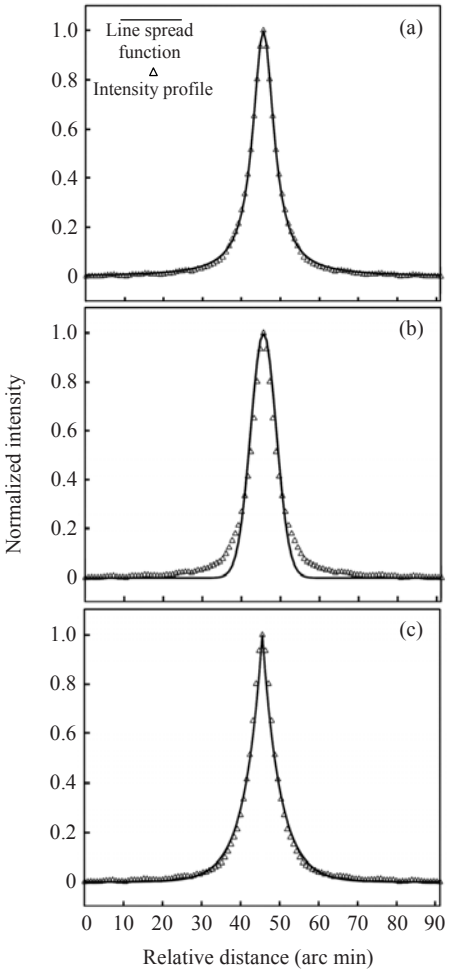

Fig.2 Examples of the same normalized double-pass line spread function fitted with (a) Lorentzian function, (b) Gaussian function, and (c) exponential function

Data analysis

The correlation coefficient (CC) between the double-pass LSF and each of the three fitted functions was calculated. The root mean square error (RMSE) of the fitted functions was determined in each subject (averaged over three images) and represented a measure of goodness of fit. A paired Student's *t*-test was used to determine the presence of a statistically significant difference in the RMSE values between the functions. Linear regression analysis was used to determine the significance of the association between the FWHM of the Lorentzian function and age. Statistical significance was accepted at $P<0.05$.

RESULTS

Based on the data in all subjects, averages for the three parameters Γ (FWHM of the Lorenztian function), σ (*SD* of the Gaussian function), and b (decay rate of the exponential function) were calculated. The mean±*SD* of Γ was (11.9±3.3) arc min (N=21). The fitting parameters σ and b, had mean±*SD* of (5.8±1.6) and (8.1±2.3) (arc min)$^{-1}$, respectively. The relatively large variation of all the three parameters indicates significant variability in the LSF shape for subjects of different ages. The relation between the FWHM of the Lorentzian fitted curve (Γ) and age of subjects is shown in Fig.3. The width of the fitted curve was significantly correlated with the subjects' ages (R=0.572, P=0.007, N=21).

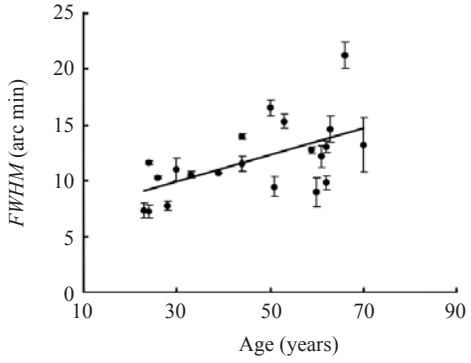

Fig.3 The relationship between the full width at half maximum (FWHM) of the Lorentzian function and age. The error bars represent the standard error (*SE*) of the means

The CC value (mean±*SD*) obtained from Lorentzian fitting (0.995±0.004) was greater than those from Gaussian fitting (0.992±0.005) and from exponential fitting (0.989±0.005). Overall, each function was highly correlated with the LSF, resulting in mean CC values greater than 0.98. The variability of CC

value attained with each function was approximately the same.

The mean±*SD* of the RMSE, representing a measure of the goodness of fit to the double-pass LSF, was calculated for the three mathematical functions, as shown in Fig.4. The mean RMSE value obtained from Lorentzian fitting (0.029±0.013) was significantly smaller than those from Gaussian fitting (0.043±0.011) (P=0.004, N=21) and exponential fitting (0.050±0.015) (P<0.001, N=21).

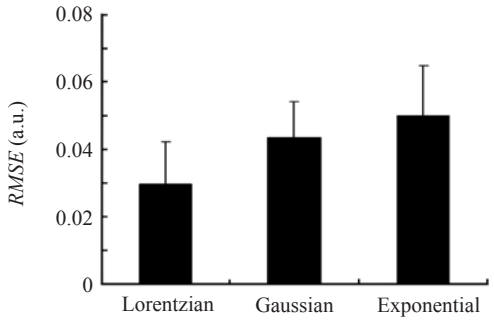

Fig.4 The mean root mean square error (RSME) for fitting the double-pass line spread function to each of the three fitted functions. Error bars represent the standard deviations (*SD*)

The RMSE values for the Lorentzian fitting (goodness of fit) derived from data in younger subjects (age range 23~39 years; average (28±5) years; N=8) were statistically compared with those in older subjects (age range 44~70 years; average (57±8) years; N=13), as shown in Fig.5. The mean RMSE in the younger subjects (0.021±0.007) was significantly lower (P=0.02) than that in older subjects (0.034±0.013), indicating that the goodness of fit was better in younger subjects.

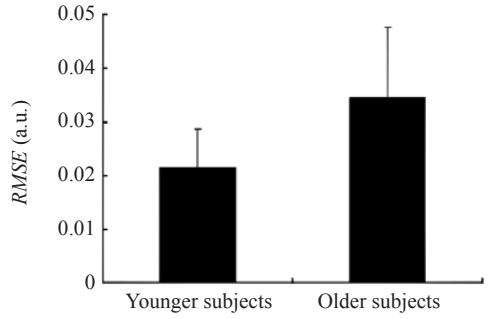

Fig.5 The mean root mean square error (RMSE) for fitting of the line spread function to the Lorentzian function in younger subjects (age range (28±5) years; *N*=8) and older subjects (age range (57±8) years; *N*=13). The error bars represent the standard deviations (*SD*)

DISCUSSION

A mathematical function that describes the LSF can serve as a model for assessing the optical performance of the eye and quantitatively characterizing retinal image quality. In the current study, the mathematical function that best characterized the double-pass LSF of healthy human eyes was found to be the Lorentzian function. The FWHM of the Lorentzian fitted curve was found to be significantly associated with subjects' ages, indicating that the LSF is broadened due to normal aging. Furthermore, the goodness of fit was different in younger and older subjects, indicating that increased aberrations or scatter due to aging in normal subjects will alter the LSF fitting function.

The Lorentzian function provided the best description of the double-pass LSF of the human eye as compared with Gaussian and exponential functions. The mean FWHM in 5 subjects (age ≤28 years) was (8.9±2.0) arc min as compared with approximately 6 arc min measured for a 6-mm pupil in 3 subjects of similar age (Campbell and Gubisch, 1966). The larger width measured in the current study may be due to the contribution of the posterior interface spread function, which caused a shift in the peak and broadening of the width of the double-pass LSF derived from the anterior interface. Numerical modeling was performed to determine the influence of the posterior interface spread function on the double-pass LSF. Assuming that the width of the anterior and posterior spread was equal to the experimentally measured mean FWHM of 8.9 arc min, a peak separation of half the FWHM resulted in a maximum double-pass LSF peak shift of approximately 2 arc min and width broadening of 3 arc min. Therefore, accounting for this factor, the adjusted double-pass LSF FWHM was estimated to be 5.9 arc min, which corresponded well with previous studies (Campbell and Gubisch, 1966) in spite of differences between the entry and exit pupil sizes.

A deconvolution method has been utilized to derive the single pass LSF from the double-pass LSF (Flamant, 1955; Westheimer and Campbell, 1962; Krauskopf, 1962), although issues with the accuracy of this technique have been raised (Artal *et al*., 1995b). However, in order to compare our results with previously published data (Flamant, 1955; Westheimer and Campbell, 1962), the same deconvolution method

was utilized to derive the single pass LSF. Like previously published studies (Flamant, 1955; Westheimer and Campbell, 1962), the single pass LSF was found to be best-fitted with the exponential function, although the inverse of mean decay constant b was measured to be (0.38±0.06) (arc min)$^{-1}$ (age ≤28 years, N=5), which was smaller than that of 0.7 (arc min)$^{-1}$ reported for a 3-mm pupil in one subject. The discrepancy in the measurements is likely due to the contribution of the posterior interface spread function as discussed above, and/or differences between the entry and exit pupil sizes.

Both the broadness and the shape of the double-pass LSF vary in dependence on light scatter, aberrations, and diffraction. As the eye ages, aberrations and scattering are increased (Ijspeert *et al*., 1990; Siik *et al*., 1992; Whitaker *et al*., 1993; van den Berg, 1995; Hennelly *et al*., 1998; Guirao *et al*., 1999; Calver *et al*., 1999; Kuroda *et al*., 2002; Fujikado *et al*., 2004), thus resulting in LSF broadening. In this study, since primarily the central region of the double-pass LSF was examined, aberrations and diffraction likely had a dominant role in determining the LSF shape. The results of the current study indicate broadening of the Lorentzian fitted curve with age, corresponding to previous studies that have reported increased aberrations due to aging in normal subjects (Hammond *et al*., 2000; Artal *et al*., 2002; 2003; Brunette *et al*., 2003; Amano *et al*., 2004). Also, the width of the LSF depends on pupil size and has been reported to vary by 1.8 arc min for pupil diameters in the range of 4.9~6.6 mm (Campbell and Gubisch, 1966). Due to the slit-lamp's stereobase angle, a minimum pupil dilation of 5 mm was necessary for imaging and thus, in the current study, the subjects' pupil sizes varied between 5 and 7 mm. The difference between the mean FWHM of the double-pass LSF of younger and older subjects was measured to be 2.9 arc min, which is larger than 1.8 arc min variation that can be attributed to changes in pupil size. Furthermore, the association between age and the LSF FWHM may have been underestimated, because older subjects have smaller dilated pupil sizes than younger subjects (Hammond *et al*., 2000), which tends to result in better image quality or a narrower LSF. Therefore, measurements under a fixed pupil size would reveal a stronger dependence of LSF FWHM on age than those obtained under variable pupil sizes.

One limitation of the current study was that the LSF was derived by projection of laser light through only one portion of the cornea and lens. Since only one specific area was sampled, the presence of non-uniformities in aberrations from other areas of the cornea and lens was not accounted for. Although this limitation likely did not influence our results in normal aging eyes, it may impact future studies in patients with cataract confined to localized regions of the lens.

In summary, identifying a mathematical function that describes the double-pass LSF is of potential value in future studies for modeling the optical performance and degradations of the eye due to cataracts and ocular diseases.

References

Amano, S., Amano, Y., Yamagami, S., Miyai, T., Miyata, K., Samejima, T., Oshika, T., 2004. Age-related changes in corneal and ocular higher-order wavefront aberrations. *Am. J. Ophthalmol.*, **137**(6):988-992. [doi:10.1016/j.ajo.2004.01.005]

Artal, P., Iglesias, I., Lopez-Gil, N., Green, D.G., 1995a. Double-pass measurements of the retinal-image quality with unequal entrance and exit pupil sizes and the reversibility of the eye's optical system. *J. Opt. Soc. Am. A: Opt. Image Sci. Vis.*, **12**(10):2358-2366. [doi:10.1364/JOSAA.12.002358]

Artal, P., Marcos, S., Navarro, R., Williams, D.R., 1995b. Odd aberrations and double-pass measurements of retinal image quality. *J. Opt. Soc. Am. A: Opt. Image Sci. Vis.*, **12**(2):195-201. [doi:10.1364/JOSAA.12.000195]

Artal, P., Berrio, E., Guirao, A., Piers, P., 2002. Contribution of the cornea and internal surfaces to the change of ocular aberrations with age. *J. Opt. Soc. Am. A: Opt. Image Sci. Vis.*, **19**(1):137-143. [doi:10.1364/JOSAA.19.000137]

Artal, P., Guirao, A., Berrio, E., Piers, P., Norrby, S., 2003. Optical aberrations and the aging eye. *Int. Ophthalmol. Clin.*, **43**:63-77.

Beckman, C., Nilsson, O., Paulsson, L.E., 1994. Intraocular light-scattering in vision, artistic painting, and photography. *Appl. Optics.*, **33**:4749-4753.

Brunette, I., Bueno, J.M., Parent, M., Hamam, H., Simonet, P., 2003. Monochromatic aberrations as a function of age, from childhood to advanced age. *Invest. Ophthalmol. Vis. Sci.*, **44**(12):5438-5446. [doi:10.1167/iovs.02-1042]

Calver, R.I., Cox, M.J., Elliott, D.B., 1999. Effect of aging on the monochromatic aberrations of the human eye. *J. Opt. Soc. Am. A: Opt. Image Sci. Vis.*, **16**(9):2069-2078. [doi:10.1364/JOSAA.16.002069]

Campbell, F.W., Gubisch, R.W., 1966. Optical quality of the human eye. *J. Physiol.*, **186**:558-578.

Chen, L., Singer, B., Guirao, A., Porter, J., Williams, D.R., 2005. Image metrics for predicting subjective image

quality. *Optom. Vis. Sci*., **82**(5):358-369. [doi:10.1097/01.OPX.0000162647.80768.7F]

Collins, M.J., Buehren, T., Iskander, D.R., 2006. Retinal image quality, reading and myopia. *Vision Res*., **46**(1-2):196-215. [doi:10.1016/j.visres.2005.03.012]

David, C.C., 1996. Lasers and Electro-Optics: Fundamentals and Engineering. Cambridge University Press, New York, NY.

Diaz-Douton, F., Benito, A., Pujol, J., Arjona, M., Guell, J.L., Artal, P., 2006. Comparison of the retinal image quality with a Hartmann-Shack wavefront sensor and a double-pass instrument. *Invest. Ophthalmol. Vis. Sci.*, **47**(4):1710-1716. [doi:10.1167/iovs.05-1049]

Flamant, M.F., 1955. Etude de la repartition de lumiere dans l'image retinienne d'une fente. *Rev. Opt.*, **34**:433-459.

Fujikado, T., Kuroda, T., Ninomiya, S., Maeda, N., Tano, Y., Oshika, T., Hirohara, Y., Mihashi, T., 2004. Age-related changes in ocular and corneal aberrations. *Am. J. Ophthalmol.*, **138**(1):143-146. [doi:10.1016/j.ajo.2004.01.051]

Guirao, A., Gonzalez, C., Redondo, M., Geraghty, E., Norrby, S., Artal, P., 1999. Average optical performance of the human eye as a function of age in a normal population. *Invest. Ophthalmol. Vis. Sci*., **40**:203-213.

Hammond, C.J., Snieder, H., Spector, T.D., Gilbert, C.E., 2000. Factors affecting pupil size after dilatation: the Twin Eye Study. *Br. J. Ophthalmol*., **84**(10):1173-1176. [doi:10.1136/bjo.84.10.1173]

Hennelly, M.L., Barbur, J.L., Edgar, D.F., Woodward, E.G., 1998. The effect of age on the light scattering characteristics of the eye. *Ophthalmic Physiol. Opt.*, **18**(2):197-203. [doi:10.1046/j.1475-1313.1998.00333.x]

Iglesias, I., Berrio, E., Artal, P., 1998. Estimates of the ocular wave aberration from pairs of double-pass retinal images. *J. Opt. Soc. Am. A: Opt. Image Sci. Vis.*, **15**(9):2466-2476. [doi:10.1364/JOSAA.15.002466]

Ijspeert, J.K., Dewaard, P.W.T., van den Berg, T.J.T.P., Dejong, P.T.V.M., 1990. The intraocular straylight function in 129 healthy-volunteers: dependence on angle, age and pigmentation. *Vision Res*., **30**(5):699-707. [doi:10.1016/0042-6989(90)90096-4]

Jones, R.C., 1958. On the point and line spread functions of photographic images. *J. Opt. Soc. Am. A: Opt. Image Sci. Vis.*, **48**(12):934-937. [doi:10.1364/JOSA.48.000934]

Karbassi, M., Magnante, P.C., Wolfe, J.K., Chylack, L.T.Jr., 1993. Objective line spread function measurements, Snellen acuity, and LOCS II classification in patients with cataract. *Optom. Vis. Sci*., **70**:956-962.

Krauskopf, J., 1962. Light distribution in human retinal images. *J. Opt. Soc. Am. A: Opt. Image Sci. Vis*., **52**(9):1046-1050. [doi:10.1364/JOSA.52.001046]

Kuroda, T., Fujikado, T., Ninomiya, S., Maeda, N., Hirohara, Y., Mihashi, T., 2002. Effect of aging on ocular light scatter and higher order aberrations. *J. Refract. Surg.*, **18**:598-602.

Liang, J., Westheimer, G., 1995. Optical performances of human eyes derived from double-pass measurements. *J. Opt. Soc. Am. A: Opt. Image Sci. Vis.*, **12**(7):1411-1416. [doi:10.1364/JOSAA.12.001411]

Navarro, R., Losada, M.A., 1995. Phase transfer and point-spread function of the human eye determined by a new asymmetric double-pass method. *J. Opt. Soc. Am. A: Opt. Image Sci. Vis.*, **12**(11):2385-2392. [doi:10.1364/JOSAA.12.002385]

Peng, Y., Lu, R., 2005. Modeling multispectral scattering profiles for prediction of apple fruit firmness. *Transactions of the Asae*, **48**:235-242.

Röhler, R., Howland, H.C., 1979. Merits of the Gaussian moment in judging optical line spread width—coment on a paper by W.N. Charman and J.A.M. Jennings. *Vision Res.*, **19**(7):847-849. [doi:10.1016/0042-6989(79)90165-2]

Shahidi, M., Yang, Y., 2004. Measurements of ocular aberrations and light scatter in healthy subjects. *Optom. Vis. Sci.*, **81**(11):853-857. [doi:10.1097/01.OPX.0000145022.74296.45]

Shahidi, M., Blair, N.P., Mori, M., Zelkha, R., 2004. Optical section retinal imaging and wavefront sensing in diabetes. *Optom. Vis. Sci.*, **81**(10):778-784. [doi:10.1097/00006324-200410000-00010]

Siik, S., Airaksinen, P.J., Tuulonen, A., 1992. Light scatter in aging and cataractous human lens. *Acta Ophthalmol. (Copenh)*, **70**:383-388.

van den Berg, T.J., 1995. Analysis of intraocular straylight, especially in relation to age. *Optom. Vis. Sci.*, **72**(2):52-59. [doi:10.1097/00006324-199502000-00003]

Westheimer, G., 1963. Optical and motor factors in the formation of the retinal image. *J. Opt. Soc. Am.*, **53**(1):86-93. [doi:10.1364/JOSA.53.000086]

Westheimer, G., Campbell, F.W., 1962. Light distribution in the image formed by the living human eye. *J. Opt. Soc. Am.*, **52**(9):1040-1045. [doi:10.1364/JOSA.52.001040]

Westheimer, G., Liang, J., 1994. Evaluating diffusion of light in the eye by objective means. *Invest. Ophthalmol. Vis. Sci*., **35**:2652-2657.

Westheimer, G., Liang, J., 1995. Influence of ocular light scatter on the eye's optical performance. *J. Opt. Soc. Am. A: Opt. Image Sci. Vis.*, **12**(7):1417-1424. [doi:10.1364/JOSAA.12.001417]

Whitaker, D., Steen, R., Elliott, D.B., 1993. Light scatter in the normal young, elderly, and cataractous eye demonstrates little wavelength dependency. *Optom. Vis. Sci*., **70**:963-968.

Yin, S., Gardner, T.W., Thomas, T.O., Kolanda, K., 2003. Light scatter causes the grayness of detached retinas: implications for vision loss in retinal detachment. *Arch. Ophthalmol.*, **121**(7):1002-1008. [doi:10.1001/archopht.121.7.1002]